

Individual Avatar Skeletal based Animation Feedback for Assisted Motion Control

Lars Lehmann¹^a, Christian Wiede²^b and Gangolf Hirtz¹^c

¹Digital Signal Processing and Circuit Technology, Chemnitz University, Reichenhainer Str. 70, Chemnitz, Germany

²Fraunhofer IMS, Finkenstr. 61, Duisburg, Germany

Keywords: Visualisation, Feedback Control, Assisted Motion Control, Motion Error Detection, 3D Realtime Animation.

Abstract: In medical training therapy (MTT), the precise execution of the training exercises is of decisive importance for the success of the therapy. Currently, a therapist has to treat up to 15 patients simultaneously on an outpatient basis. Recently an assistance system that can assess both the quantity and the quality of movement was developed. A feedback system models target-oriented recommendations for actions and communicates them directly to the patient. A hardware accelerated visualisation system using OpenGL and GLSL shaders was realised to animate a real-time rendered 3D mesh connected to an extracted motion skeleton. An avatar visualises the error by colouring the body regions with traffic light trenches. The individualisation of the underlying three-dimensional avatar increases the willingness of the patients to participate in the exercises which they perform autonomously without the supervision of therapists.


1 INTRODUCTION


After a hip operation, the treated persons have to complete a rehabilitation phase lasting several weeks in a special MTT centre. In the MTT, up to 15 patients are monitored simultaneously by a therapist (Nitzsche, 2018). Therefore, there is no guarantee that the therapist will have a constant overview of every single patient in the rehabilitation centre. This lack of control can have a negative effect, since in the unobserved moments movement errors are performed by the patient, which, above a certain number, have an extremely negative effect on the treatment (Lösch, 2019). It is necessary to support the overburdened therapist staff with a self-sufficient, markerless assistance system that monitors the patient's movements and immediately warns them of movement errors. Currently, we use for the assistance system a depth sensor, which is able to extract the patient's skeleton and evaluate his movement sequence by means of artificial intelligence. Subsequently, it is necessary to present the data to the patient in a suitable way. This feedback have to be clear, explicit and immediate, as the evaluation of the movement takes place immedi-


ately and during the training. Moreover, the results must also be transmitted and displayed in real time.

Our proposed approach includes the animation of an individual, three-dimensional wireframe model in real time. For this purpose, a freely selectable three-dimensional avatar is coupled with a previously extracted skeleton so that its movement is projected directly onto the attached mesh. In addition to the network animation, the affected areas of the body are coloured according to the recorded error in a known three-part colour scale, which reflects the current state of the movement error. Due to the large number of individual parameters to be transmitted and their combination in shader stages, a standard system such as Unity (Smith, 2015) is not the means of choice for the representation. Therefore, the realisation was carried out directly and hardware-oriented on a graphics card with the help of OpenGL and GLSL under the aspect of real-time mapping (Wolff, 2018).

In the following Section 2, systems already in circulation that deal with the rehabilitation aspect are evaluated and presented. In Section 3 the proposal work by us regarding a real-time animation of skeleton-coupled three-dimensional meshes is explained and the necessary steps are explained. In order to realise the colouration of mesh segments, certain algorithms are used in Section 4. The implemented solution has already been extensively tested in

^a <https://orcid.org/0000-0001-9778-8479>

^b <https://orcid.org/0000-0002-2511-4659>

^c <https://orcid.org/0000-0002-4393-5354>

practice and the relevant surveys and experiences will be discussed in the following Section 5, before the future planned extensions will be mentioned in Section 6.

2 RELATED WORK

Due to demographic change, there has been an increase in the number of older people in society, and at the same time there is a lack of movement therapists in MTT. The problem can be countered with the help of the assistance system, which is able to determine the patient's motions and quantify it (J. Richter and Hirtz, 2017). For this purpose it is sensible to introduce a visual feedback system that motivates people to go into strenuous therapy (E. Velloso and Gellersen, 2013)(Kwon and Gross, 2005)(Zhao, 2014). Their work deals with the development of a suitable feedback system with a special focus on the model representation of the visualisation necessary for the transmission of monitored movements. Velloso et al. (E. Velloso and Gellersen, 2013) uses markers to capture the following motion analysis. The implementation of a visualisation is limited to the text output in a 2D real-time image. According to this study, these hints of the action display have already proven to be useful automation. For an extended work of this approach, Kwon and Gross (Kwon and Gross, 2005) presented a system that can be present on a monitor. A skeleton is visualised, on which a user can follow during the execution of his exercises. The system guides as an expert through a given training and analyses the movement. Depending on the evaluation, the skeleton is coloured in traffic light colours in case of a motion error. Another rehabilitation system with motion control is presented by Zhao et al. (Zhao, 2014). A 3D view of a model with a standard game development platform (Smith, 2015) is outlined. The model embodies the test subjects and helps them to get involved in the therapy. Movement becomes more motivating and thus more successful. The approach pursues the goal of increasing the success of therapy and supports the automated detection of movements. The errors of the model are not coloured yet and the additional textual hints for a avoidance of the occurred error are missing.

For our method, we combine all these approaches and extend them. In particular, the representation of the animation model, its segmentation and the body-related error colouring have been improved. Furthermore, a significant improvement of details and the individuality in the representation of freely selectable

avatars for real-time animations were carried out and evaluated.

3 SKELETON-BASED ANIMATION

The selected wireframe model presented to the volunteers has to be animated in order to display the patient's movement in real time. For this aim, it is connected to a sensor-generated skeleton model, which is presented in subsection 3.1. This skeleton, which is constantly updated and reflects the movement of the patient, causes an equal animation movement in the coupled mesh. Skeleton and model thus form an inseparable unit, inform about the current movement and offer an immersively individualised rehabilitation procedure.

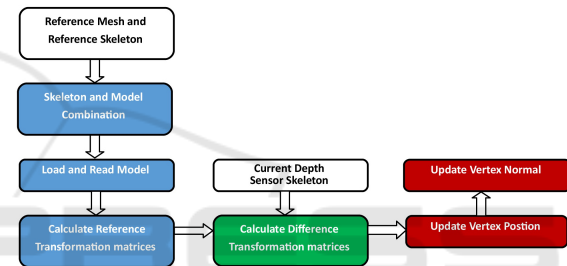


Figure 1: A skeletal wireframe model animation requires several processing steps: 1) one-time calculation on the CPU (blue), 2) dynamic recurring CPU calculations (green) and 3) hardware intensive GPU calculations (red).

The animation of a wireframe model oriented on skeleton points requires computational extensive implementation steps. Since real-time capability must be guaranteed, the visualisation process cannot only be realised on the CPU, but must also include the GPU. Figure 1 illustrates all necessary steps. In each individual step, calculations are carried out, which must be available in the following section in order to ensure proper skeletal wireframe model animation. Some of these calculations are performed only once on the CPU (the calculation of the static reference transformations of the loaded skeleton model), others are also performed on the CPU (the calculation of the dynamic difference transformation between the current and static skeleton model) at each current incoming skeleton change and others are performed on the GPU (the calculation of the new vertex positions of the triangle mesh and the corresponding normal) at each individual render step.

3.1 Static Animation Calculation

First the reference skeleton system is connected to the reference mesh. This is performed once on the CPU. In order to make the connection, the model is first rigged and then skinned (Crespo, 2003).

The purpose of rigging is to create a duplicate corresponding to the existing extraction skeleton. This duplicate is scaled and shifted so that it fits exactly to the existing mesh. There are several 3D modeling tools on the market that are able to perform this. Thus a bone hierarchy is created with Blender (Blain, 2019), which connects all associated child bones starting from a root bone in order to adapt the skeletal system.

The following skinning of the mesh includes the assignment of bones involved in the animation to a vertex describing the mesh surface. The forces of attraction of the bones to the vertex are calculated. The forces are very large when the vertex is positioned in the immediate vicinity of the bone and decrease with increasing distance. A nearby bone has a high force of attraction on the vertex and other distant bones. In the proposed assistance system, up to eight possible participation bones are noted.

The rigged skinned model available in Blender is then exported to our visualisation system with all available vertex data. The transformation matrices of the reference skeleton system are as well calculated. However, each bone has its own bone coordinate system. For the animation, however, we need these single values in relation to the root coordinate system and its transformation matrix m_r , which is the only one already statically adopted. For this purpose, all matrices of the chained children's bones are multiplied down to the root bone and the new reference system of the bone under consideration is created. For the complete iteration of the entire skeleton, the depth of the adjacent bone d of each bone b has to be considered first.

$$b[i].m_r = m_r \cdot b[i].m_r \quad \text{for } i = 0, \dots, d \quad (1)$$

The matrices m_r of each bone that are now available are required for the difference adjustment to the dynamically occurring skeletal changes that result from movement of the test person and are saved for the entire duration of the training (Huey, 2014). These root matrices m_r must be updated if the reference wireframe model or the reference skeleton model changes. In these cases, the vertex attribute coupling is no longer suitable because the corresponding geometry has been modified.

3.2 Dynamic Animation Calculation

When the test person moves, the depth sensor extracts a new skeleton. This is compared with the previously calculated reference system in subsection 3.1 describing the standard position and its motion difference (Mukundan, 2012) is determined.

Since these calculations only refer to the bone system to be described by the sparse skeleton data in which each individual bone is described by a start and end point, they can also be performed dynamically on the CPU without a noticeable loss of performance being measurable. Therefore the skeletal connection of the incoming bone data has to be known in order to recalculate the reference. For each incoming bone, its start point s and end point e are set. For the required updated 3D transformation matrices m_t of the bone, the vector difference es_Δ and their length l are determined. A transformed direction vector td of the bone is then calculated.

$$\begin{pmatrix} x \\ y \\ z \end{pmatrix}_{es_\Delta} = \begin{pmatrix} x \\ y \\ z \end{pmatrix}_e - \begin{pmatrix} x \\ y \\ z \end{pmatrix}_s \quad (2)$$

$$\begin{pmatrix} x \\ y \\ z \end{pmatrix}_{td} = \begin{pmatrix} x \\ y \\ z \end{pmatrix}_{es_\Delta} \cdot \frac{1}{l} \quad (3)$$

The rotation between the static reference delta res_Δ , i.e. the difference between the end vector and the start vector of the reference skeleton from capital 3.1 and the now available transformation direction td is described by the quaternion q (Beutelspacher, 2010).

$$q = \text{rot} \left(\begin{pmatrix} x \\ y \\ z \end{pmatrix}_{res_\Delta}, \begin{pmatrix} x \\ y \\ z \end{pmatrix}_{td} \right) \quad (4)$$

The final transformation matrix m_f of the bone results from the transformation of the quaternion into a 3x3 matrix.

3.3 Hardware-accelerated Dynamic Animation Calculation

The surface animation of the wireframe model connected to the skeleton is calculated with a shader program on the GPU to ensure real-time capability. Due to its architecture, the GPU is able to execute graphics operations much faster than the less specialised CPU.

The following calculation steps must be applied per frame (Movania, 2013) for each individual surface point, i.e. each individual vertex of the entire grid, in order to realise the correct animation per render step.

The first step is to transfer the index values b_j of the bones important for the vertex to the shader, which are already provided in the subsection 3.1. It can be computed how many bone weights act on the considered vertex. By iterating over the array it can be determined which bone influences the vertex. Since there are eight possible influencing segments in the system, this interval is examined to determine the number of weights w_c .

$$w_c = \sum_{i=0}^7 b_j[i] \begin{cases} +0 & \text{if } 255 \\ +1 & \text{otherwise} \end{cases} \quad (5)$$

In addition, the total weight w_s , which denotes the individual bones involved in the vertex, is calculated by iteratively adding up the individual weight values. For this aim, the exact weight arrays b_w from subsection 3.1 in the shader are needed.

$$w_s = \sum_{i=0}^{w_c} b_w[i] \quad (6)$$

Consequently, the number of weights w_c has been determined, an iteration of the next steps for the new vertex position is carried out.

The index i_b of the useful bone is derived from the array of available bone indices.

$$i_b = b_j[i] \quad \text{for } i = 0, \dots, w_c \quad (7)$$

The determination of the position transformation vector p_Δ is the difference between the considered static vertex position p and the static starting point b_{rsp} , the associated reference bone segment resulting from the iteration, which was previously forwarded to the shader.

$$\begin{pmatrix} x \\ y \\ z \end{pmatrix}_{p_\Delta} = \left(\begin{pmatrix} x \\ y \\ z \end{pmatrix}_p - \begin{pmatrix} x \\ y \\ z \end{pmatrix}_{b_{rsp}[i_b]} \right) \quad (8)$$

When the current transformation matrix m_f of the bone determined dynamically on the CPU is multiplied by the position transformation vector p_Δ , the current rotation displacement vector r_Δ of the vertex results.

$$\begin{pmatrix} x \\ y \\ z \end{pmatrix}_{r_\Delta} = \left(\begin{bmatrix} a_{11} & \cdots & a_{13} \\ \vdots & \ddots & \vdots \\ a_{31} & \cdots & a_{33} \end{bmatrix}_{m_f[i_b]} \cdot \begin{pmatrix} x \\ y \\ z \end{pmatrix}_{p_\Delta} \right) \quad (9)$$

For the final determination of the new vertex position a weight factor f_w is needed which results from the

division of the current weight value b_w and the total weight of the bones w_s .

$$f_w = \left(\frac{b_w[i]}{w_s} \right) \quad \text{for } (i = 0, \dots, w_i) \quad (10)$$

The starting point of the current proband skeleton bone b_{sp} is added to the rotation displacement vector r_Δ and the result is multiplied by the weight factor f_w . The sum of all iteration steps of the skeletal bones involved is the new position p_n of the vector shifted by the skeleton animation to be rendered.

$$\begin{pmatrix} x \\ y \\ z \end{pmatrix}_{p_n} = \sum_{i=0}^{w_c} \left(\left(\begin{pmatrix} x \\ y \\ z \end{pmatrix}_{b_{sp}[i_b]} + \begin{pmatrix} x \\ y \\ z \end{pmatrix}_{r_\Delta} \right) \cdot f_w \right) \quad (11)$$

For the new normal n_n the procedure is relatively similar. Here, too, the single iterations are summarized. Thereby the single values result from the multiplication of the current dynamic bone transformation matrix m_f , the vertex normal n and the weight factor f_w . The normal n_n necessary for the illumination is transferred to the next vertex colouring shader step for processing.

$$\begin{pmatrix} x \\ y \\ z \end{pmatrix}_{n_n} = \sum_{i=0}^{w_c} \left(m_f[i_b] \cdot \begin{pmatrix} x \\ y \\ z \end{pmatrix}_n \cdot f_w \right) \quad (12)$$

4 COLOURATION OF MESH SEGMENTS

If the assistance system that evaluates the movement detects an error in the exercise sequence, this refers to a specific area of the patient's body. By marking this body segment in colour, the patient is immediately aware of where the movement error occurs and the error can be avoided during the next exercise. The traffic light colouring, known from road traffic, visualise the patient whether it is an error (red), a warning (yellow) or whether the procedure was carried out correctly (green or standard mesh colour).

The sequence of such segmentation colouring is shown in the Figure 2. The reference mesh and the corresponding reference skeleton are the starting point for the colour-coded error display. After the skeleton and the 3D avatar have been connected, the segmentation of the skeletonised surface can take place. Subsequently, the current motion errors occurring on the skeleton can be displayed directly on the mesh. The error attributes are dynamically updated

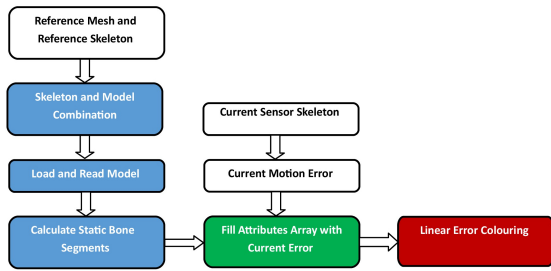


Figure 2: The segmented linear error colouring is calculated statically (blue) and dynamically (green) on the CPU and passed as a vertex attribute to the fast GPU (red).

and forwarded to the shader units (Crespo, 2003) of the processing chain.

4.1 Bone Bound Mesh Segmentation

The motion errors are detected by the assistance system by comparing the instantaneous skeletal motion with the position of a reference skeleton. In order to display the deviations on the mesh, the bone position on the surface grid of the mesh have to be closed. Therefore, each surface vertex is assigned exactly the bone that is selected as the main bone for it on the basis of the distance and the corresponding attraction weight. The data provided by the reference system is sufficient to perform a single segmentation directly on the CPU. The resulting data can be used with dynamic processes, since the mesh does not re-segment during animation.

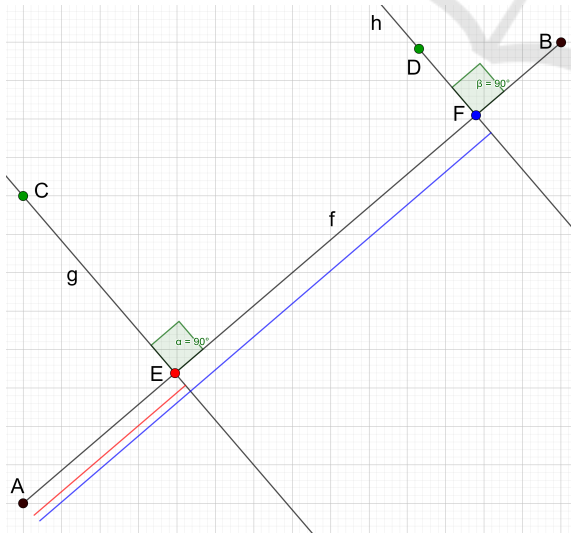


Figure 3: The linear segmentation of the bone AB by the perpendicular foot point calculation of F and H through the surface vertices D and F .

The two points C and D in Figure 3 are surface vertices of the 3D avatar. The standard Gaussian dis-

tribution of weights corresponding to the principal weight in the middle of the bone is to be converted into a linear distribution over the bone line so that the colouration can be performed evenly from bone beginning to bone end, i.e. from A to B . Once all nodes v of the wireframe model have been processed and all required data extracted, the bone index b_{imax} of the largest weight value b_{wmax} is determined for each node from the corresponding field b_w to calculate the main bone of the node.

$$b_{wmax} = \sum_{i=0}^7 \max(b_w[i]) \quad \text{foreach}(v) \quad (13)$$

$$b_{imax} = i \quad \text{if } b_{wmax} \quad (14)$$

C and D are thus assigned to the bone AB . After the involved vertices have been defined, the perpendicular lines g and h are dropped onto the bone line AB and their intersections E and F are calculated.

$$\begin{pmatrix} x \\ y \\ z \end{pmatrix}_{AB} = \left(\begin{pmatrix} x \\ y \\ z \end{pmatrix}_B - \begin{pmatrix} x \\ y \\ z \end{pmatrix}_A \right) \quad (15)$$

$$v_u = \begin{pmatrix} (C.x - A.x) \cdot AB.x \\ (C.y - A.y) \cdot AB.y \\ (C.z - A.z) \cdot AB.z \end{pmatrix} \quad (16)$$

$$u = \frac{v_u.x + v_u.y + v_u.z}{AB.x^2 + AB.y^2 + AB.z^2} \quad (17)$$

$$\begin{pmatrix} x \\ y \\ z \end{pmatrix}_E = \begin{pmatrix} A.x + u \cdot AB.x \\ A.y + u \cdot AB.y \\ A.z + u \cdot AB.z \end{pmatrix} \quad (18)$$

For the above equations (17) and (18) the intersection vector E is calculated as an example. For F and its reference point D as well as for all other vertices belonging to the bone this intersection point has to be determined as well.

The quotient between the length of the subvector AE and the length of the total vector AB gives the percentage share of AE with respect to AB , i.e. exactly the desired linear factor f_s for the desired segmentation. The proportion of AE (red) to the total distance AB is less than that of AF (blue).

$$f_s = \frac{\text{length}(AD)}{\text{length}(AB)} \quad (19)$$

Using the factor f_s the reference mesh can be coloured segment by segment. In order to do this, a four-dimensional vector is assigned to each surface vertex of the mesh, which contains its colour.

$$\begin{pmatrix} x \\ y \\ z \\ a \end{pmatrix}_{colour} = \begin{pmatrix} f_w \\ 0.0 \\ 1.0 - f_w \\ 1.0 \end{pmatrix} \quad (20)$$

Using the example of this red-blue colouring approach, the following results are obtained for linear segment colouring for various freely selectable grid models.

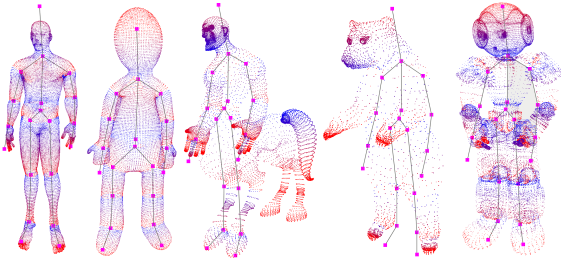


Figure 4: Linear staining of bone segments for various individual wire mesh models.

4.2 Segmented Motion Error Coloring

Once the bone segmentation has been calculated, it can be used to clearly represent a movement error in the animated model. Since the entire surface has to be considered, the graphic pipeline is dependent on the colour-processing layer of the GPU. Thus, the real-time requirement can also be fulfilled during the processing of 3D vertices.

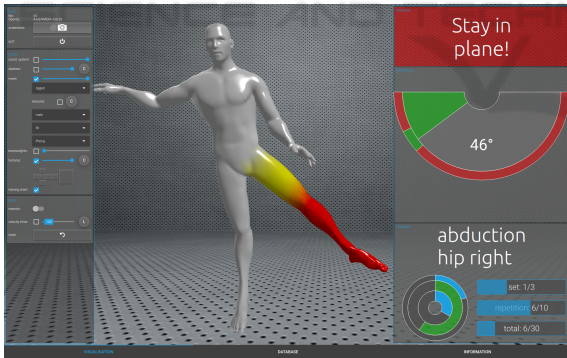


Figure 5: A real-time animated wireframe model in MTT that colours the error segments.

This is converted in the visualisation unit into a shader attribute, which will be filled with three sub-segments per skeletal bone which hold a suitable colour for the visualisation. Thus, a bone can have three different colours if it supports the error estimation and the entire skeleton is indexed coloured. Figure 5 shows a linear colouration for a deviation detected on the right leg.

For the realisation of the visualisation, each bone of the skeletal system used is iterated and checked

whether there is an error for this index in one of the three segments s_i of the error attribute v_e . If this is the case, the desired colour and its intensity are calculated.

This is carried out by using the static percentage factor of the linear weight distribution f_s calculated on the CPU in subsection 4.1, to determine in which segment area of the bone the vertex can be localised. The value is now used to calculate the vertex colour v_c over a sine-cosine-distribution.

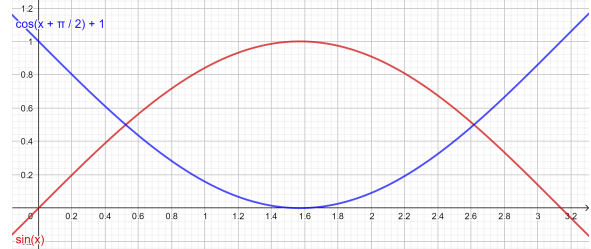


Figure 6: The colouration of the vertex consists of the normalised sum of cosine and sine values, which are determined by the distance factor f_w .

It is distinguished whether the factor is above or below the value 0.5 in order to determine the correct cosine fraction for the first summand. In the Figure 6 this function is marked by the blue, shifted cosine curve.

$$v_c = (1.0 - \cos(\Pi/2 + (-f_w * \Pi))) \cdot v_e[s_i] \quad (21)$$

$$v_c = (1.0 + \cos(\Pi + (2(-f_w * \Pi/2)))) \cdot v_e[s_i] \quad (22)$$

If $f_s < 0.5$ the equation 21 is used in any other case equation 22.

If the first summand is determined, the second sinusoidal summand, in Figure 6 the red curve, is calculated for the normalized sum and added to the previous one to determine the final three-dimensional colour vector.

$$v_c = \sin(f_w * \Pi) \cdot v_e[s_i] + v_c \quad (23)$$

This sum always generates values between 0 to 1 and determines the three RGB values of the colour vector that estimates how the colour value is composed for the position vector.

5 RESULTS AND DISCUSSION

An assistance system has been developed to help MTT patients to perform their movements in an orderly and targeted manner. The core of the system

is the rope pull on which the movements are carried out. The patient stands in front of a depth sensor, which extracts the skeletal data and performs a motion analysis. The results are visualised in real time on a display belonging to the assistance system. Both the coloured animation mesh and the textual hints associated with the movement are visualised.

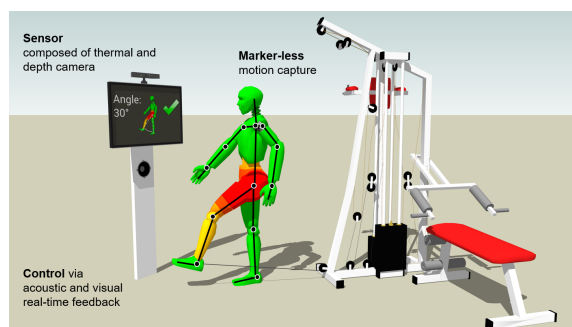


Figure 7: The design of the assistance system for the study consists of a wire rope hoist, depth sensor and a display monitor (J. Richter, 2017).

The C++ standardised toolkit Qt was used for the realisation of the assistance system. This framework is characterised by increased flexibility in GUI creation. Qt has the declarative programming language QML, whereby individual GUIs can be created with the help of a JSON-based metalanguage. During the implementation of the visual feedback, a real-time realisation was a particularly noteworthy aspect. Since the patients had to be informed immediately about their wrong movements, which should already avoid their error during the next movement execution, a GLSL shader implementation became unavoidable. Even meshes beyond the 100,000 individual vertices could be displayed in real time. Also the animation with different single models and the change of the models was realised. Thus the motivation of the patients could be increased, because they preferred different animation models. Since OpenGL was already used for the animation, the coloration of the bone segments could be implemented in a further GLSL shader step on the fragment side. This implementation meets the necessary real-time requirements, which require a frame rate of 25 frames per second, and rounds off the desired assistance system in terms of information density. For the application's humanoid standard mesh, which requires 146754 vertices to be rendered per visualization step, the frame rate is 60 frames per second, where one AMD ATI Radeon RX Vega M GL graphics card is used.

A user acceptance study was conducted to test the system in clinical practice. The aim was to investigate how the visual feedback system encouraged and motivated patients to perform the movements to be

trained properly and how the visual design was perceived. For this purpose, the assistance system was tested in a clinical facility, for patients with a new hip implant. 15 subjects completed a three-week rehabilitation program and trained with the assistance system under therapeutic supervision. Patients were then asked to complete a standardised questionnaire with twelve questions and five possible answers.

In the survey, the system was predominantly assessed positively. The evaluation of the movement feedback, which was important for the question of the paper, and the indications of an autocorrection were mostly understandable and helpful (Nitzsche, 2018).

In addition, the error frequencies were evaluated over the duration of the therapy. The aim was to determine whether the patient's movements could be improved during the training period with the help of the assistance system. This also shows that the error rate monitored by the assistance system decreased by more than 50% (Lösch, 2019).

6 CONCLUSION AND FUTURE WORK

A visual feedback was created for the movement therapy, in which it is possible to select an individual avatar for the display. The movements were analysed and evaluated. Errors were coloured according to their importance in traffic light colours on the previously calculated bone segments. This allows patients to see immediately where the error occurred. In order to evaluate the assisted therapy system, a user study was carried out with 15 subjects. The results indicates a high user acceptance. The independent evaluation of the recorded training results showed a noticeable gain in health-promoting movements.

In future the integration of real scanned individual characters would promote immersion. Of course, the creation of the models would have to be feasible as a sideline and without too much time expenditure.

The monitoring of the control should also extend to other body regions. Both the hands and the face could be integrated into the motion monitoring. In addition, an automatic system to record reference movements have to be implemented. Thereby, the therapists could store a new motion sequence at any time.

The integration of the complete system into a virtual reality environment would have an increased immersion. The limitation that is associated with a fixed location feedback system would be abolished. It would no longer be necessary to realign the display device for body rotated exercise changes.

REFERENCES

- Beutelspacher, A. (2010). *Lineare Algebra*. Vieweg+Teubner Verlag, Wiesbaden, 7th edition.
- Blain, J. (2019). *The Complete Guide to Blender Graphics: Computer Modeling and Animation*. Taylor and Francis Ltd, London, 5th edition.
- Crespo, D. S. (2003). *Core Techniques and Algorithms in Game Programming*. New Riders Publishing, San Francisco, 1st edition.
- E. Velloso, A. B. and Gellersen, H. (2013). Motionma: motion modelling and analysis by demonstration. In *CHI '13, Proceedings of the SIGCHI Conference on Human Factors in Computing Systems*. ACM.
- Huey, L. B. (2014). Paper templates. In *Example-based Rigging and Real-time Animation of Characters with Linear Skinning Models*. ETD Collection.
- J. Richter, C. W. and Hirtz, G. (2017). Motion error classification for assisted physical therapy - a novel approach using incremental dynamic time warping and normalised hierarchical skeleton joint data. In *ICPRAM 2017*. Semantic Scholar.
- J. Richter, C. W. and Hirtz, G. (2017). Assisted Motion Control in Therapy Environments Using Smart Sensor Technology: Challenges and Opportunities. In *9. AAL-Kongress. Ambient Assisted Living*.
- Kwon, D. Y. and Gross, M. (2005). Combining body sensors and visual sensors for motion training. In *ACE '05, Proceedings of the 2005 ACM SIGCHI International Conference on Advances in computer entertainment technology*. ACM.
- Lösch, C. (2019). Paper templates. In *Validation of an assistance system for motion analysis*. German Journal of Sports Medicine.
- Movania, M. M. (2013). *OpenGL Development Cookbook*. Packt Publishing, Birmingham, 1st edition.
- Mukundan, R. (2012). *Advanced Methods in Computer Graphics: With examples in OpenGL*. Springer, Berlin, 2nd edition.
- Nitzsche, N. (2018). *Assistierte Bewegungskontrolle in der Rehabilitation durch intelligente Sensortechnologie*. readbox unipress, Münster, 1st edition.
- Smith, M. (2015). *Unity 5.x Cookbook: More than 100 solutions to build amazing 2D and 3D games with Unity*. Packt Publishing, Birmingham, 1st edition.
- Wolff, D. (2018). *OpenGL 4 Shading Language Codebook*. Packt Publishing, Birmingham, 3rd edition.
- Zhao, W. (2014). Combining body sensors and visual sensors for motion training. In *5th IEEE International Conference on Software Engineering and Service Science*. IEEE.